Korean J. Chem. Eng., 40(4), 903-909 (2023)
DOI: 10.1007/s11814-023-1390-6

pISSN: 0256-1115
eISSN: 1975-7220

A microfluidic platform for simulating stem cell migration using *in vivo*-like gradients of stem cell mobilizer

Jin Kim*,‡, Jinyoung Kim*,‡, Hyun-Ji Park*,,‡, Eun Je Jeon*, and Seung-Woo Cho*,†**

*Department of Biotechnology, Yonsei University, Seoul 03722, Korea
**Department of Molecular Science and Technology, Ajou University, Suwon 16499, Korea
(*Received 26 September 2022 • Revised 26 December 2022 • Accepted 29 December 2022*)

Abstract−Stem cell mobilization by cytokines and peptide drugs contributes to wound healing in injured tissues. Owing to the short half-life of cytokines and short peptides *in vivo*, precisely predicting the *in vivo* therapeutic efficacy of stem cell mobilizers is difficult using current *in vitro* models. To address this problem, we developed a multichannel microfluidic device with diffusion barriers to recapitulate drug gradients in an *in vivo*-like environment. We investigated the effects of Substance P (SP), a stem cell mobilizer, on the migration of human bone marrow-derived mesenchymal stem cells (BM-MSCs) in the microfluidic chip, which replicated *in vivo* drug gradients. Simulations of SP concentration indicated that our microfluidic chip established SP gradients in migration channels, unlike the existing scratch model for cell migration assays. The scratch model did not distinguish the effects of SP with a short half-life and PEGylated SP with an extended half-life on BM-MSC migration, whereas the microfluidic system demonstrated that PEG-SP affected BM-MSC migration more than SP. Furthermore, the microfluidic chip allowed accurate quantification of the distance and direction of BM-MSC migration. Our microfluidic system could be useful for the precise evaluation of drugs associated with cell migration and mobilization.

Keywords: Microfluidic Chip, Cell Migration, Stem Cell Mobilization, Substance P, Drug Gradient

INTRODUCTION

Endogenous stem cells mediate *in situ* wound healing in defective tissues [1-3]. Several factors, such as granulocyte colony stimulating factor (G-CSF) and granulocyte-macrophage colony stimulating factor (GM-CSF), are known to facilitate endogenous stem cell mobilization from the bone marrow to the circulating peripheral blood, which leads to the enrichment of stem cells in injured tissue [4-7]. Novel therapeutic factors that recruit and mobilize endogenous stem cells to defective target tissues will enable highly effective cell-free tissue regeneration regimens. Thus, *in vitro* test platforms that precisely evaluate stem cell migration using novel factors are required. There are several existing *in vitro* techniques to analyze drug-induced cell migration, including the scratch assay and the transwell assay [8-12]. However, these techniques have several limitations regarding controlling and evaluating cell mobilizer effects. A scratch assay on a regular cell culture dish or plate can evaluate cell migration according to the type and concentration of the drug, but cannot differentiate between sizes of drug molecules because drug gradients are minimally reconstituted in this assay [13]. Transwell-based cell invasion assays can evaluate the chemotaxis of cells based on the size of the testing drug molecule. However, this assay cannot precisely assess the *in vivo*-like behaviors of the testing molecules because of the absence of a three-dimensional (3D) diffusion barrier, which is required to maintain the gradient of molecules [14,15]. The pore size of the transwell membrane and the gravitational forces often limit cell mobilizer effects due to steep but unstable molecular gradient formation and size limitations of applicable cells and cell mobilizers. Furthermore, cell migratory direction between upper and lower wells delimits live cell imaging. The micromixer-based microfluidic chip provides one way to overcome low controllability and poor visibility of conventional cell migration assays. In a previous study, the microfluidic platform enabled the linear and stable gradient of the chemoattractant perpendicular to the channel flow, and thus successfully demonstrated neutrophil chemotaxis to interleukin 8 gradient [16]. Another study incorporated extracellular matrix-based hydrogel to a 3D microfluidic chip to represent *in vivo* microenvironment [17]. This method efficiently recapitulated *in vivo*-like 3D dynamics of chemotactic cell behavior.

To overcome the limitations of conventional assays for the analysis of cell migration, we developed a microfluidic chip platform with a 3D diffusion barrier that simulates *in vivo* cell migration using stem cell mobilizers. Owing to the presence of a 3D collagen hydrogel as a diffusion barrier, our microfluidic chip allows the detection of differences in stem cell migration depending on the molecular size of drugs, which has been difficult to evaluate precisely in the existing *in vitro* cell migration assays. Here, we simulated *in vivo* stem cell migration of Substance P (SP) in the microfluidic chip. SP, a short polypeptide of 11 amino acids (RPKPQQFFGLM), is known to augment the mobilization of stem and progenitor cells from the bone marrow to circulating blood and subsequently promote wound healing in defective peripheral tissues [18-20]. To address the limited therapeutic efficacy of SP owing to its short

†To whom correspondence should be addressed.
E-mail: seungwoocho@yonsei.ac.kr
‡These authors contributed equally to this work.

half-life *in vivo* (Approximately 1 min) [21-23], we previously synthesized a polyethylene glycol (PEG)-conjugated SP with an extended half-life and increased stability [23]. Thus, our microfluidic chip simulated how the chemotaxis is altered by the different sizes of the SP and PEG-SP molecules, and these results were compared with those from the conventional scratch assay. Indeed, the difference in the migration of human bone marrow-derived mesenchymal stem cells (BM-MSCs) mediated by SP and PEG-SP could only be validated in the microfluidic chip with a 3D hydrogel barrier channel, while the conventional scratch assay did not differentiate BM-MSC migration by SP and PEG-SP. This was likely due to a lack of drug gradients, as predicted by simulation analysis. The effect of the SP antagonist was also confirmed in the microfluidic chip. Treatment with the neurokinin 1 receptor antagonist (RP67580), a known SP antagonist [24,25], significantly reduced the migration of BM-MSCs treated with SP and PEG-SP. Overall, these results demonstrated that the microfluidic chip reported in this study could effectively simulate and predict *in vivo* stem cell migration using a stem cell mobilizer and its inhibitor.

METHODS

1. Design and Fabrication of the Microfluidic Chip

A microfluidic chip was designed to have five channels to create drug concentration gradient so that stem cell migration could be analyzed: Channel I (factor channel), Channel II (diffusion barrier), Channel III (gradient channel), Channel IV (cell channel), and Channel V (medium channel) (Fig. 1(a)). The microfluidic device was fabricated using a soft lithography method with polydimethylsiloxane (PDMS; Dow Corning, Auburn, MI, USA). The PDMS-patterned membrane was molded into the designed shape and was sterilized by autoclaving. The membrane was then bonded to a sterilized cover glass by oxygen plasma treatment (60 W, 40 s; Femto Science, Seoul, Korea). The procedure for preparing the microfluidic chip for the analysis of BM-MSCs migration by SP and PEG-SP treatments is illustrated in Fig. 1(b). First, 50 μg/mL collagen I (Corning, Bedford, MA, USA) in phosphate-buffered saline was coated onto the surface of the channels to promote cell adhesion. BM-MSCs (passage numbers 7-8; Lonza, Bazel, Switzerland) were seeded onto Channel IV at a density of 1×10^7 cells/mL and incubated for 2 h to allow cell attachment. To prevent rapid diffusion of SP and to create an SP concentration gradient, a pre-gel solution of collagen I was added to Channel II 30 min before SP treatment. Collagen cross-linking was induced to form a 3D collagen hydrogel that acted as a diffusion barrier. Dulbecco's Modified Eagle Medium (DMEM; Thermo Fisher Scientific, Waltham, MA, USA) supplemented with 10% (v/v) fetal bovine serum (FBS; Thermo Fisher Scientific), 1% (v/v) penicillin/streptomycin (Thermo Fisher Scientific), and basic fibroblast growth factor (bFGF; 20 ng/mL, R&D Systems, Minneapolis, MN, USA) was added to the channels. The culture medium was changed every 24 h.

2. Synthesis of PEG-SP and Measurement of SP Half-life

PEG-SP was synthesized as described in a previous study [19]. Methoxy PEG-succinimidyl succinate (250 mg/mL, 10 kDa mPEG-

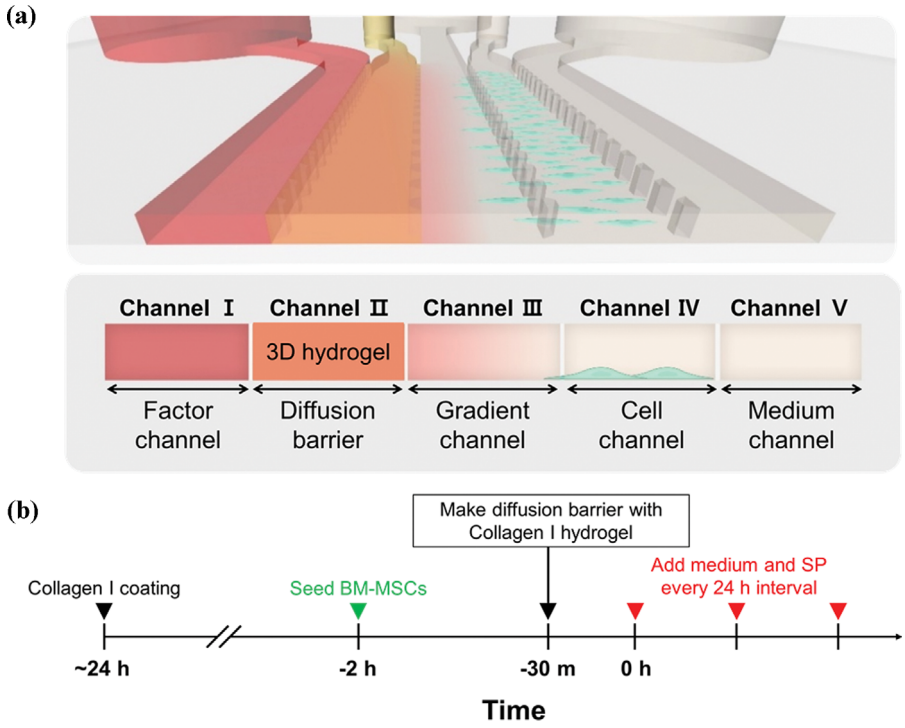

Fig. 1. Design of microfluidic chip and schematic for stem cell migration experiment. (a) Configuration of microfluidic chip; Channel I (factor channel for administration of drugs such as SP, PEG-SP, and RP67580), Channel II (diffusion barrier with 3D collagen type I hydrogel), Channel III (gradient channel for drug gradients and cell migration), Channel IV (cell channel for cell seeding and start point of cell migration), and Channel V (medium channel to provide medium supply). (b) Time-table for microfluidic chip preparation and cell migration experiment.

SS; SunBio, Anyang, Korea) and SP (10 mg/mL; Anygen, Kwangju, Korea) dissolved in 10 mM Tris buffer (pH 7.5) were mixed in equal volumes and stirred overnight at 4 °C. The reaction mixture was purified using an Amicon ultra-centrifugal filter system (NMWL 10 kDa; EMD Millipore, Billerica, MA, USA). The half-lives of SP and PEG-SP were examined in a culture medium of DMEM supplemented with 10% (v/v) FBS and 1% (v/v) penicillin/streptomycin. SP and PEG-SP were added to 100 μL of the culture medium at a concentration of 5 nmol and incubated for 72 h at 37 °C and 5% CO_2. The amount of remaining SP was measured at predetermined time points using an SP Parameter Assay Kit (#KGE007, R&D Systems). The concentrations of SP and PEG-SP were calculated through conversion to molar mass using their corresponding molecular weights (1,347.63 g SP/mol and 21,347.63 g PEG-SP/mol).

3. Cell Migration Test in a Scratch Model

Cell migration in a conventional scratch assay was tested as a control. Eight-well chamber slides (Thermo Fisher Scientific) were used for the scratch assay. The chamber slide was coated with 50 mg/mL collagen I for 2 h and the BM-MSCs were then seeded onto the chamber slide at a cell density of 1×10^6 cells/mL. They were incubated in DMEM supplemented with 10% (v/v) FBS, 1% (v/v) penicillin/streptomycin, and 20 ng/mL bFGF overnight to allow cell adhesion. The next day, the BM-MSC monolayer was deprived of serum for 4 h and scraped with a straight line using a 200 μL pipette tip. The culture medium was replaced with fresh serum-free medium containing either SP or PEG-SP. After 12 h of incubation, the migration distance of the BM-MSCs within the scraped region was analyzed using ImageJ 1.49v software (National Institutes of Health, Bethesda, MD, USA).

4. Cell Migration Test in a Microfluidic Chip System

SP or PEG-SP (1 pmol) was added to Channel I (factor channel) to induce BM-MSC migration in the microfluidic chip. The migration of BM-MSC from Channel IV (cell channel) to Channel III (gradient channel) was analyzed at 0, 12, 24, 48, and 72 h of culture. To observe how the SP antagonist affected BM-MSC migration in the microfluidic chip, 10 nM of RP67580 (Sigma-Aldrich) was added to Channel I along with SP or PEG-SP. The cell culture medium containing SP or PEG-SP, with or without RP67580, was replaced every 24 h. At each of these analysis time points, the cells were fixed with 10% formalin and stained with TRITC-conjugated phalloidin (Sigma-Aldrich). The distance and angular distribution of migration were quantified using ImageJ 1.49v software.

5. Computational Simulation of SP Concentration

A computational program, COMSOL Multiphysics software (COMSOL Inc., Burlington, MA, USA), was used to simulate SP concentration in the cell culture slide and the microfluidic chip. The model was simulated using the microfluidic module of COMSOL Multiphysics software with the following parameters was used: density of culture medium, 1,030 kg/m^3 [26]; dynamic viscosity of culture medium, 0.0025 Pa·s [26]; SP diffusion coefficient in aqueous solution, 2.83×10^{-12} m^2/s [27]; porosity of hydrogel, 0.9 [28]; maximum SP degradation rate, 8.29×10^{-12} mol/cell·s (calculated based on [20]); Michaelis-Menten constant k_m of SP, 190 μM [20]. To match the conditions for the cell tests, the initial SP concentration was set to 0.1 mM in the overall domain in the scratch test and in Channel I of the microfluidic chip.

6. Statistical Analysis

All statistical analyses were performed using the GraphPad Prism 9 software (GraphPad, San Diego, CA, USA). Data are shown as mean±standard deviation (SD) unless otherwise stated. An unpaired Student's *t*-test was applied, and *p*-values<0.05 were considered significant in all tests.

RESULTS AND DISCUSSION

1. Microfluidic Chip Preparation for Stem Cell Migration by SP and PEG-SP

A microfluidic chip was fabricated with PDMS using soft lithography to replicate *in vivo* drug gradients and cell migration. Intravenously injected SP circulates in the bloodstream before reaching target sites like bone marrow through diffusion barriers such as 3D extracellular matrices [29]. SP gradients across diffusion barriers affect the mobilization of BM-MSCs into other peripheral tissues. To simulate the *in vivo* behavior of SP, we designed a microfluidic chip with a 3D hydrogel diffusion barrier made from collagen type I, the main component of connective tissue. The chip was fabricated with five microchannels in the following order: (1) drug administration channel (Channel I), (2) 3D hydrogel channel as a diffusion barrier (Channel II), (3) drug gradient channel for cell migration (Channel III), (4) cell seeding channel (Channel IV), and (5) medium channel (Channel V) (Fig. 1(a)). A schedule of the cell migration test within the microfluidic chip is shown in Fig. 1(b). To facilitate cell adhesion, a collagen type I coating was applied to all channels 24 h before drug administration. BM-MSCs were then seeded onto Channel IV 2 h before drug treatment, and then a collagen I hydrogel diffusion barrier was formed in Channel II. Finally, SP and PEG-SP were administered to Channel I, and the culture medium was added to Channel V. Because PEG-SP has two PEG moieties (10 kDa) within the SP molecule, the molecular weight of PEG-SP (21.347 kDa) is higher than that of SP (1.347 kDa) (Fig. 2(a)). PEGylation is one of the most efficient strategies to extend the half-lives of the peptides and proteins [30]. PEG arms on PEG-SP conjugates can protect SP from enzymatic degradation and hydrolytic cleavage [31,32]. Moreover, the amphiphilic nature of PEG-SP may allow micelle formation with SP core and PEG shell, which renders PEG-SP more resistant to degradation [33,34]. Indeed, the half-life of PEG-SP was up to 40 h longer than that of SP (1 h) under physiologically relevant conditions (DMEM culture medium supplemented with 10% FBS) (Fig. 2(b)). Overall, PEGylation of SP not only increases the molecular weight but also protects SP from degradation, leading to the extended half-life of SP and differences in diffusion profiles and rates between SP and PEG-SP over time. Thus, we speculate that when SP and PEG-SP pass through Channel II (3D hydrogel diffusion barrier), different concentration gradients are formed in Channel III (gradient channel).

2. Comparison of Stem Cell Migration between the Scratch Model and Microfluidic Chip

To verify the feasibility of our microfluidic chip as an *in vitro* platform for precisely evaluating stem cell migration by SP and PEG-SP, we compared BM-MSCs migration by SP and PEG-SP in

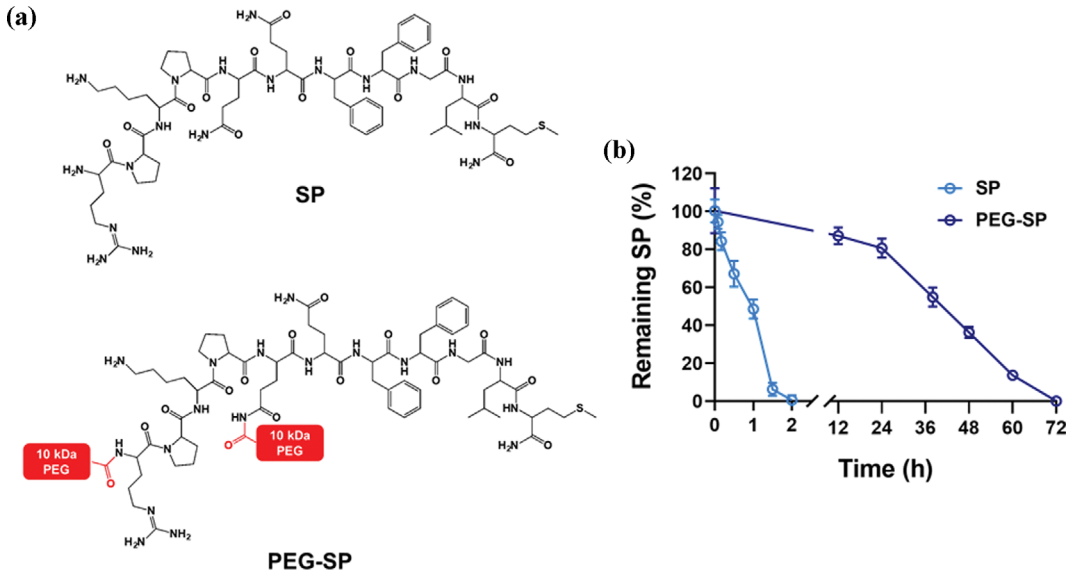

Fig. 2. Characterization of SP and PEG-SP. (a) The chemical structure of SP and PEG-SP. For synthesis of PEG-SP, SP peptide (RPKPQQFFGLM) was chemically conjugated with PEG moieties to the arginine (R) and lysine (K) residues. (b) Degradation profiles of SP and PEG-SP in culture medium (DMEM supplemented with 10% (v/v) FBS) at 37 °C (n=4).

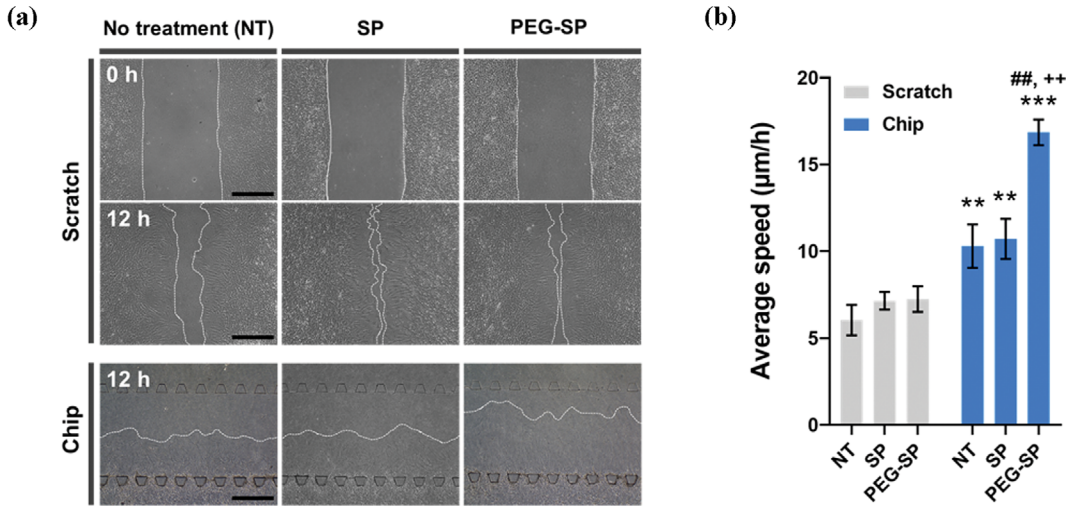

Fig. 3. The migration of human BM-MSCs in scratch model and microfluidic chip system. (a) Microscopic observation of human BM-MSC migration 12 h after SP or PEG-SP treatment. White dotted lines indicate the location of migrating cells (scale bars=500 μm). (b) Average migration speed of human BM-MSCs over 12 h in the scratch model (chamber slide) and microfluidic chip (n=3; **p<0.01, ***p<0.001 vs. each corresponding group in scratch assay, ##p<0.01 vs. NT group in chip assay, ++p<0.01 vs. SP group in chip assay).

the microfluidic chip with that in the conventional scratch assay. Interestingly, the scratch model did not show differences in the extent of BM-MSC migration between the SP and PEG-SP treatments, as shown in Fig. 3(a). In contrast, the microfluidic chip with a diffusion barrier of 3D collagen I hydrogel could distinguish the enhanced migration of BM-MSCs treated with PEG-SP, compared to those treated with SP (Fig. 3(a)). Likewise, the average migration speed of BM-MSCs was not significantly different between the SP and PEG-SP groups in the scratch assay; however, in the microfluidic chip, the migration speed of BM-MSCs treated with PEG-SP was much higher than that of cells treated with SP (Fig. 3(b)). This discrepancy could be attributed to the 3D diffusion barrier in the microfluidic platform reconstituting different gradients of SP and PEG-SP. As SP and PEG-SP appeared to diffuse throughout the entire well in the scratch model without a 3D hydrogel barrier, distinct concentration gradients between SP and PEG-SP were not formed, leading to insignificant differences in stem cell migration by SP and PEG-SP treatments. However, when SP and PEG-SP were administered into Channel I of the microfluidic chip, they passed through Channel II with the 3D diffusion barrier of the collagen hydrogel, ultimately leading to concentration gradients of SP and PEG-SP in Channel III. In this situation, SP was likely to decompose more rapidly than PEG-SP before being transferred to Channel IV. This resulted in the varying effects of SP and PEG-SP

on stem cell migration in the microfluidic chip.

3. Simulation of the SP Gradient in Scratch Model and Microfluidic Chip

The simulation predicted that the different migration extents of BM-MSC in the scratch model and microfluidic chip were caused by different SP diffusion rates and concentration gradients. In the well with the scratch, SP rapidly diffused throughout the well, leading to the absence of SP gradients (Fig. 4(a)). This indicates that

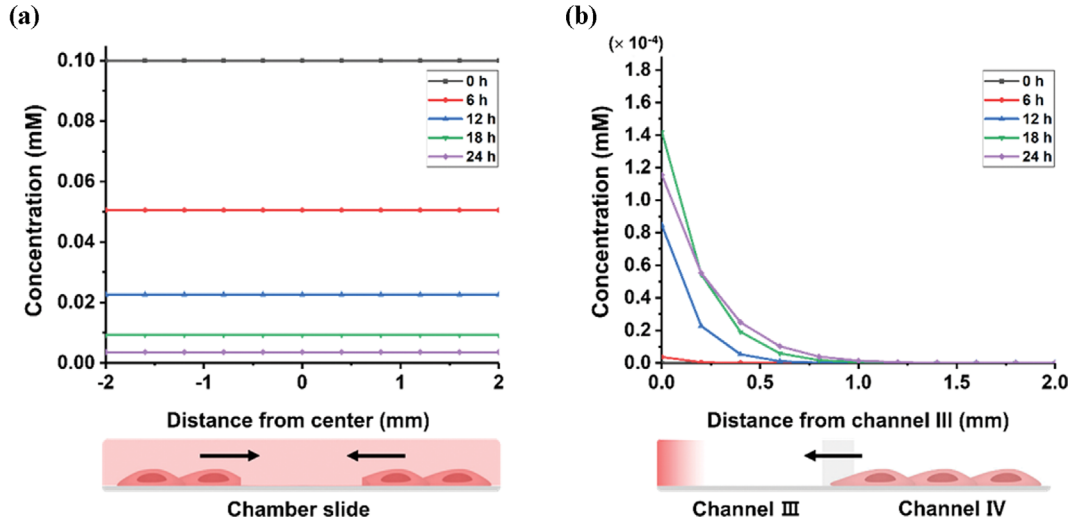

Fig. 4. Simulation of SP concentration gradients in scratch model and microfluidic chip system. (a) SP concentration in the cell culture slide for scratch assay. (b) SP concentration in the Channel III and Channel IV of the microfluidic chip. Simulation analysis data indicate SP concentrations in both assays every 6 h up to 24 h. Schematic illustrations below the graphs show the direction of BM-MSC migration (black arrows) due to SP concentration gradients.

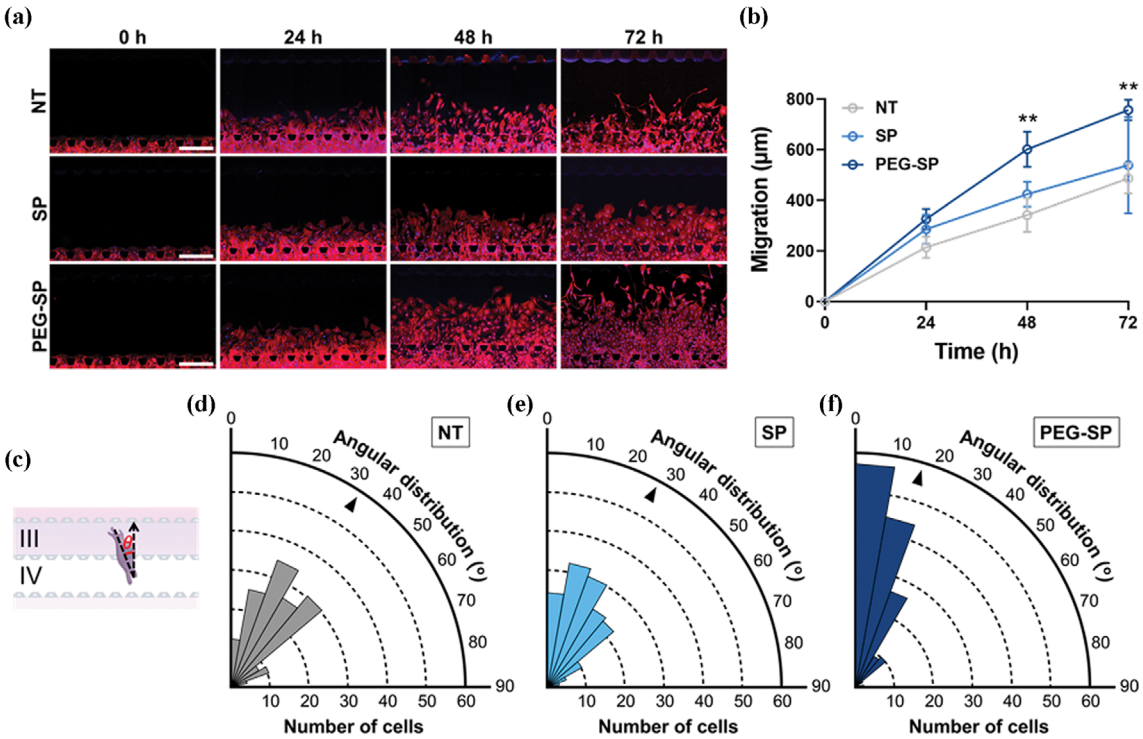

Fig. 5. Migration of human BM-MSCs treated with SP and PEG-SP in microfluidic chip. (a) Migration of phalloidin-labelled BM-MSCs treated with SP or PEG-SP in the microfluidic chip (24, 48, and 72 h of culture, scale bars=500 μm). (b) Migration distance quantified from the fluorescence images of phalloidin-labelled BM-MSCs in each group. NT denotes the no treatment group (n=3; **p<0.01 vs. NT and SP groups). (c) Measurement of the angular distribution of the direction of cell migration from Channel IV to Channel III in the microfluidic chip. (d)-(f) Angular distribution of human BM-MSC migration in (d) NT, (e) SP, and (f) PEG-SP groups. Average angular distribution in each group is marked with a black triangle.

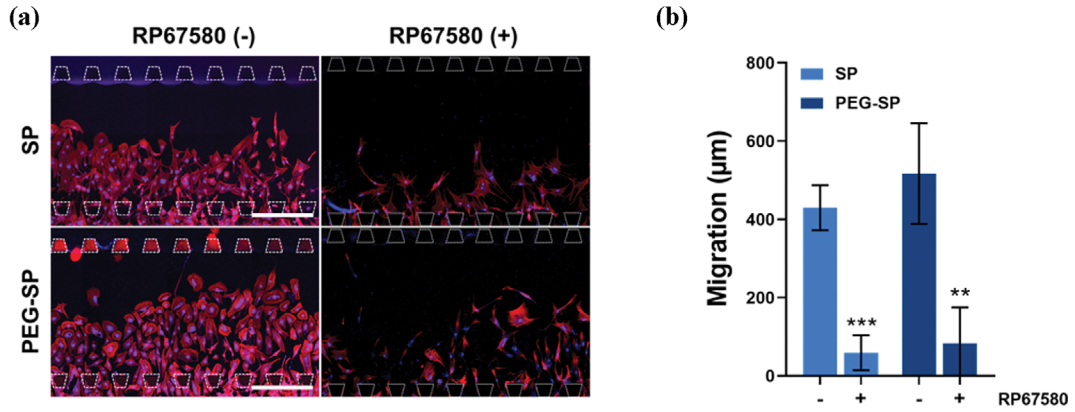

Fig. 6. Effect of antagonist on the migration of human BM-MSCs treated with SP and PEG-SP in the microfluidic chip. (a) Migration of SP- or PEG-SP-treated BM-MSCs exposed to SP antagonist (10 nM RP67580) in the microfluidic chip (72 h of culture, scale bars=500 μm). BM-MSCs were labelled with phalloidin. (b) Migration distance of BM-MSCs quantified from the fluorescence images of phalloidin-labelled BM-MSCs in each group (n=3, **p<0.01, ***p<0.001 vs. each corresponding RP67580 (−) group).

SP in the scratch model could bind to SP membrane receptors on BM-MSCs within minutes, and consequently induce a certain level of cell migration (Fig. 3). In contrast, SP concentration gradients were created according to the location of the microfluidic chip with a 3D diffusion barrier (Fig. 4(b)). Since SP diffusion in microfluidic system with 3D diffusion barrier is not as fast as much as that in scratch model, it seems that SP degradation became more prominent in the 3D microfluidic chip and, consequently, the effect of SP without PEGylation on BM-MSC migration was negligible (Fig. 3(b)). Given the large difference in molecular weights of SP and PEG-SP, their different diffusion behaviors in microfluidic system were also likely to result in such differential BM-MSC migration effects. Although computational analysis of PEG-SP diffusion behaviors was not conducted in our study, we assume that the gradients of PEG-SP formed through 3D collagen hydrogel and its prolonged half-life could induce BM-MSC migration for extended period in comparison to SP. Therefore, the effects of stem cell mobilizers administered *in vivo*, especially those with a short half-life such as SP, can be better understood using our microfluidic system than with conventional migration assays.

4. The Effect of Stem Cell Mobilizer in Microfluidic Chip

We further examined stem cell migration by SP and PEG-SP throughout the culture time in the microfluidic chip. The migration of BM-MSCs from Channel IV to Channel III after three days was significantly increased by PEG-SP treatment compared with no treatment or SP treatment (Fig. 5(a)). The prolonged effect of PEG-SP owing to its extended half-life was demonstrated in the microfluidic chip. BM-MSCs treated with PEG-SP migrated further than those with SP treatment or no treatment (Fig. 5(b)). SP treatment did not significantly enhance the migration distance of BM-MSCs compared to no treatment. Unmodified SP likely decomposed during transfer through the 3D hydrogel barrier due to its short half-life. The angular distribution, which indicates the direction of cell movement from Channel IV to Channel III, was examined in the microfluidic chip (Fig. 5(c)). BM-MSCs treated with PEG-SP exhibited an average angular distribution value of approximately 15°, while cells treated with SP or without any treatment showed average angular distribution values of approximately 30° (Fig. 5(d)-(f)). A larger number of BM-MSCs treated with PEG-SP was found to move with directional propensity toward Channel III. This indicates that different SP gradients formed during the diffusion of SP and PEG-SP through the 3D hydrogel barrier affect the efficiency of stem cell migration for each treatment.

5. The Effect of SP Antagonist in Microfluidic Chip

The effects of drug antagonists often need to be examined to identify and validate their mode of action. Thus, we investigated the effect of an SP antagonist (RP67580) on BM-MSC migration using a microfluidic chip system (Fig. 6). Upon exposure to RP67580 administered through Channel I, migration of BM-MSCs treated with SP or PEG-SP significantly decreased (Fig. 6(a) and (b)), indicating the SP antagonist adversely affected stem cell migration in the microfluidic system. We found that the migration distance of BM-MSCs cotreated with PEG-SP and RP67580 was reduced to a level similar to that of BM-MSCs cotreated with SP and RP67580 (Fig. 6(b)). These data demonstrate that small molecules, such as RP67580, diffused through the 3D hydrogel barrier and negated the effect of SP gradients on stem cell migration in the microfluidic system.

CONCLUSIONS

A microfluidic chip containing five microchannels and a 3D collagen diffusion barrier was tested for evaluating stem cell migration using a stem cell mobilizer (SP) and its derivative (PEG-SP), which has an increased molecular size and extended half-life. Conventional methods, such as the scratch assay, did not distinguish between the efficacy of SP and PEG-SP for stem cell migration, while the microfluidic chip enabled precise simulation of enhanced stem cell migration with PEG-SP by replicating *in vivo* SP gradients using a 3D diffusion barrier. The microfluidic chip can also quantify the cell migration speed and direction along the SP gradients. In addition, differences in cell migration, according to the presence or absence of antagonists, were observed in the microfluidic chip. Overall, our microfluidic platform can be utilized for more

accurate *in vitro* evaluation of drugs and substances that affect cell migration and mobilization for tissue regeneration and vascularization.

ACKNOWLEDGEMENTS

This work was supported by the Samsung Research Funding & Incubation Center of Samsung Electronics under project number SRFC-TC2003-03.

CONFLICT OF INTEREST

The authors declare no competing financial interest.

REFERENCES

1. T. H. Kao, Y. C. Lin, P. H. Lee, C. W. Lin, P. H. Chen, T. S. Tai, Y. C. Chang, M. H. Chou, C. Y. Chang and C. K. Sun, *Tissue. Eng. Regen. Med.*, **17**, 671 (2020).
2. S. Kim, O. J. Kwon, J. Lee, J. Kim, T.-h. Kim and K. Kim, *Biotechnol. Bioprocess Eng.*, **26**, 335 (2021).
3. Y.-C.Yang, Q.-H. Hong, K. F. Lei and A. C.-Y. Chen, *BioChip J.*, **15**, 243 (2021).
4. J. Kim, N. K. Kim, S. R. Park and B. H. Choi, *Tissue. Eng. Regen. Med.*, **16**, 59 (2019).
5. I. Petit, M. Szyper-Kravitz, A. Nagler, M. Lahav, A. Peled, L. Habler, T. Ponomaryov, R. S. Taichman, F. Arenzana-Seisdedos, N. Fujii, J. Sandbank, D. Zipori and T. Lapidot, *Nat. Immunol.*, **3**, 687 (2002).
6. C. Savitri, J. W. Kwon, V. Drobyshava, S. S. Ha and K. Park, *Tissue. Eng. Regen. Med.*, **19**, 617 (2022).
7. L. To, D. Haylock, P. Simmons and C. Juttner, *Blood*, **89**, 2233 (1997).
8. E. Baez-Jurado, O. Hidalgo-Lanussa, G. Guio-Vega, G. M. Ashraf, V. Echeverria, G. Aliev and G. E. Barreto, *Mol. Neurobiol.*, **55**, 5377 (2018).
9. M. L. De Ieso and J. V. Pei, *Biosci. Rep.*, **38**, BSR20180698 (2018).
10. O. K. Hwang, Y. W. Noh, J. T. Hong and J. W. Lee, *Tissue. Eng. Regen. Med.*, **17**, 335 (2020).
11. S. S. Omar Zaki, L. Kanesan, M. Y. D. Leong and S. Vidyadaran, *Cell. Biol. Int.*, **43**, 1201 (2019).
12. X. Tian, L. Zhang, Y. Jiao, J. Chen, Y. Shan and W. Yang, *J. Cell. Biochem.*, **120**, 3765 (2019).
13. G. Shabestani Monfared, P. Ertl and M. Rothbauer, *Pharmaceutics*, **13**, 793 (2021).
14. K. P. Goetsch and C. U. Niesler, *Anal. Biochem.*, **411**, 158 (2011).
15. M. H. Olsen, G. M. Hjorto, M. Hansen, O. Met, I. M. Svane and N. B. Larsen, *Lab Chip*, **13**, 4800 (2013).
16. N. L. Jeon, H. Baskaran, S. K. W. Dertinger, G. M. Whitesides, L. Van De Water and M. Toner, *Nat. Biotechnol.*, **20**, 826 (2002).
17. Y. Shin, S. Han, J. S. Jeon, K. Yamamoto, I. K. Zervantonakis, R. Sudo, R. D. Kamm and S. Chung, *Nat. Protoc.*, **7**, 1247 (2012).
18. H. S. Hong, J. Lee, E. Lee, Y. S. Kwon, E. Lee, W. Ahn, M. H. Jiang, J. C. Kim and Y. Son, *Nat. Med.*, **15**, 425 (2009).
19. H.-J. Park, S. Kim, E. J. Jeon, I.-T. Song, H. Lee, Y. Son, H. S. Hong and S.-W. Cho, *J. Ind. Eng. Chem.*, **78**, 396 (2019).
20. G. Andersson, L. J. Backman, A. Scott, R. Lorentzon, S. Forsgren and P. Danielson, *Br. J. Sports Med.*, **45**, 1017 (2011).
21. R. A. Skidgel, S. Engelbrecht, A. R. Johnson and E. G. Erdös, *Peptides*, **5**, 769 (1984).
22. J. J. Bowden, A. M. Garland, P. Baluk, P. Lefevre, E. F. Grady, S. R. Vigna, N. W. Bunnett and D. M. McDonald, *Proc. Natl. Acad Sci.*, **91**, 8964 (1994).
23. H. J. Park, R. Kuai, E. J. Jeon, Y. Seo, Y. Jung, J. J. Moon, A. Schwendeman and S. W. Cho, *Biomaterials*, **161**, 69 (2018).
24. C. Garret, A. Carruette, V. Fardin, S. Moussaoui, J.-F. Peyronel, O. J.-C. Blanchard and P. M. Laduron, *Proc. Natl. Acad Sci.*, **88**, 10208 (1991).
25. K. Ikeda, K. Miyata, A. Orita, H. Kubota, T. Yamada and K. Tomioka, *Neurosci. Lett.*, **198**, 103 (1995).
26. H. Moghadas, M. S. Saidi, N. Kashaninejad and N. T. Nguyen, *Drug Deliv. Transl. Res.*, **8**, 830 (2018).
27. U. L. Khatun, A. Gayen and C. Mukhopadhyay, *Glycoconj J.*, **31**, 435 (2014).
28. W. H. Fissell, C. L. Hofmann, N. Ferrell, L. Schnell, A. Dubnisheva, A. L. Zydney, P. D. Yurchenco and S. Roy, *Am. J. Physiol. Renal. Physiol.*, **297**, F1092 (2009).
29. D. Van den Brand, L. F. Massuger, R. Brock and W. P. Verdurmen, *Bioconjug. Chem.*, **28**, 846 (2017).
30. J. S. Suk, Q. Xu, N. Kim, J. Hanes and L. M. Ensign, *Adv. Drug Deliv. Rev.*, **99**, 28 (2016).
31. C. S. Fishburn, *J. Pharm. Sci.*, **97**, 4167 (2008)
32. R. Visentin, G. Pasut, F. M. Veronese and U. Mazzi, *Bioconjug. Chem.*, **15**, 1046 (2004).
33. T. Wymore and T. C. Wong, *Biophys. J.*, **76**, 1213 (1999).
34. C. Ruan, L. Liu, Y. Lu, Y. Zhang, X. He, X. Chen, Y. Zhang, Q. Chen, Q. Guo, T. Sun and C. Jiang, *Acta Pharm. Sin. B*, **8**, 85 (2018).